Engine Control of a Downsized Spark Ignited Engine: from Simulation to Vehicle

Guenael Le Solliec, Fabrice Le Berr, Guillaume Colin, Gilles Corde, Yann Chamaillard

Oil & Gas Science and Technology – Rev. IFP, Vol. 62 (2007), No. 4, pp. 555-572

DOI : 10.2516/ogst: 2007057

IFP International Conference
Rencontres Scientifiques de l'IFP

New Trends on Engine Control, Simulation and Modelling
Avancées dans le contrôle et la simulation des systèmes Groupe Moto-Propulseur

Engine Control of a Downsized Spark Ignited Engine: from Simulation to Vehicle

G. Le Solliec[1], F. Le Berr[1], G. Colin[2], G. Corde[1] and Y. Chamaillard[2]

1 Institut français du pétrole, IFP, 1 et 4 avenue de Bois-Préau, 92852 Rueil-Malmaison Cedex - France
2 Laboratoire de Mécanique et d'Énergétique, 8 rue Léonard de Vinci, 45072 Orléans Cedex 2 - France
e-mail: guenael.le-solliec@ifp.fr - fabrice.le-berr@ifp.fr - guillaume.colin@univ-orleans.fr - gilles.corde@ifp.fr

Résumé — Contrôle d'un moteur essence suralimenté à cylindrée réduite : de la simulation au véhicule — La sévérisation des normes européennes en termes de réduction de la consommation et des émissions de polluants conduit à une sophistication des concepts moteurs et des contrôles associés. Depuis quelques années la réduction de la cylindrée moteur est une solution majeure sur un moteur essence à allumage commandé pour atteindre ces objectifs. Afin de garder de bonnes performances et un bon agrément de conduite, ce concept de réduction de cylindrée est alors associé sur un moteur essence à injection directe à une suralimentation adaptée et des déphaseurs continus d'arbre à came. L'un des objectifs principaux d'un contrôle en structure couple est l'observation et le contrôle des masses enfermées dans le cylindre. Pour obtenir une bonne réponse en couple, et a fortiori de bonnes performances et un bon agrément de conduite, la masse d'air enfermée doit être parfaitement contrôlée via le papillon d'admission d'air et la vanne de décharge du turbocompresseur. En fonction de pressions d'admission et d'échappement, les déphaseurs vont permettre, soit de contrôler les gaz brûlés dans le cylindre afin de réduire la consommation et les émissions de polluants, soit la masse d'air balayée pour améliorer les temps de réponse en transitoire lors des phases de suralimentation. Dans cet article, nous proposons une approche basée sur la simulation. Le premier objectif est la conception d'observateurs des masses enfermées dans le cylindre, non mesurables. La méthode est basée sur l'utilisation d'un modèle moteur 0D haute fréquence, qui a été validé sur un large nombre de points statiques et de situations transitoires issus d'essais au banc moteur. Ce modèle permet alors de concevoir des observateurs boucle ouverte basés sur réseaux de neurones. Le comportement dynamique du modèle moteur haute fréquence permet également la conception d'un contrôle multi-variable et non-linéaire de la boucle d'air suivant des trajectoires adéquates de masses enfermées (air et gaz brûlés). Enfin, le contrôle moteur complet peut être développé et validé en simulation et sur une plateforme temps réel Software-In-the-Loop avant la validation et calibration complète au banc. Finalement, la structure couple complète a été intégrée dans le véhicule. A partir du modèle moteur 0D, un modèle véhicule complet a été implémenté sur une plateforme temps réel afin de valider l'intégration du contrôle moteur et concevoir la couche véhicule. L'objectif principal est alors la supervision des consignes (couple, richesse, efficacité) selon l'état du moteur (démarrage, ralenti, demande conducteur, coupure) et les stratégies de mise en action.

Abstract — Engine Control of a Downsized Spark Ignited Engine: from Simulation to Vehicle — *Tightening European standards on fuel consumption and pollutant emissions reduction lead to a sophistication of engine concepts and associated control. Since few years, downsizing (reduction of the engine displacement) appears as a major way to achieve those requirements for spark ignition engines. Efficient*

performance and drivability can be then achieved with a direct injection downsized engine with turbocharging and Variable Camshaft Timing (VCT). One of the major issues of the torque-oriented control is in-cylinder mass observation and control. To have an efficient torque response, the in-cylinder trapped mass, adjusted by the throttle and the waste gate, must be controlled with accuracy according to performance and drivability requirements. Depending on admission and exhaust pressures, the twin VCT will allow to control in-cylinder burned gases rate to reduce fuel consumption and pollutant emissions, and air scavenging to improve transient speed response. Another major issue is in-cylinder trapped mass and air scavenging prediction for AFR control. In this paper, we propose a model-based approach to achieve those engine control issues. The first challenge is to design accurate observers for non-measurable variables (in-cylinder burned gases and trapped air mass). The method is based on a complex high frequency 0D engine model, which has been validated on a large range of engine operating points and transient operations based on test bed results. Then, this model permits to design and learn open-loop nonlinear static observers of in-cylinder masses (based on neural network). The static and dynamic behavior of high frequency 0D engine model allows to achieve design of dynamic and closed-loop in-cylinder mass observation and prediction, multivariable and non-linear control of air path according to in-cylinder mass trajectory (trapped air mass & recirculated gases rate). Then, the complete engine control can be developed and validated on simulation and on a real time Software-In-the-Loop platform based on high frequency 0D engine model, before a complete validation and calibration on test bed. Finally, the complete torque-oriented engine control has been integrated on vehicle. From 0D engine model, a complete vehicle model has been set on real-time platform in order to validate engine control integration and design vehicle layout. The major issue is then supervision of engine control set points (torque, AFR, efficiency) according to engine states (start, idle, driver request, cut-off) and warm-up strategies.

INTRODUCTION

Engine technologies must more and more satisfy goals of minimizing fuel consumption and pollutant emission while keeping performance and drivability. A solution for reducing the fuel consumption is to improve engine efficiency. To this end, *IFP* has developed an innovative downsizing approach, combining several well known technologies: direct injection, turbocharging and variable valve timing [1]. Starting from a standard four cylinders engine with direct injection (2 liters Renault F5R), *IFP* reduced the displacement to 1.8 liters. The use of a smaller capacity engine operating at higher engine loads needs a well adapted turbocharger (Mono-scroll type) to reach performances while reducing fuel consumption. To take advantages of all the potentialities, the engine is equipped with twin variable camshaft timing (VCT), for intake and exhaust valves. This system can improve the engine on different aspects:

- Control of residual burned gases at low load to minimize fuel consumption and pollutant emissions.
- Control of scavenging at high load to reduce residual burnt gases and cylinder temperature in order to avoid knock and to improve combustion efficiency.
- Reduction of turbo-lag duration during transient by increasing mass flow rate through the turbine.

With the multiplication of complex actuators and the need for satisfying conflicting objectives, advanced engine control is therefore necessary to obtain an efficient torque control [2]. This paper's contribution is a global presentation of the torque-based engine control issues and development for this downsized SI engine.

The first section presents the methodology adopted in this project. A first challenge was to use a well adapted simulation-based process in order to well-understand engine dynamics and relevant variables to be controlled while limiting time development and real test facilities use.

A classical engine control with feed-forward commands and PID controllers becomes more and more difficult to tune, because of the system nonlinearities and dynamics. In the next section, an advanced torque-based control scheme and its main issues is presented. A major contribution is design of observers and non-linear controllers for unmeasured relevant variables: in-cylinder trapped air mass and burned gases mass.

In order to fully validate *IFP* downsizing approach, engine and *IFP* control system have been integrated in a demonstration car, a VelSatis Renault. The last section presents the vehicle layout development managing engine states, driver requests, drivability and warm-up strategies.

1 SIMULATION-BASED PROCESS

1.1 Methodology and Tools

The chosen platform for control development is Matlab/simulink because of its simulation and control design features. RTW and xPC Target toolboxes are also used for code generation and rapid prototyping.

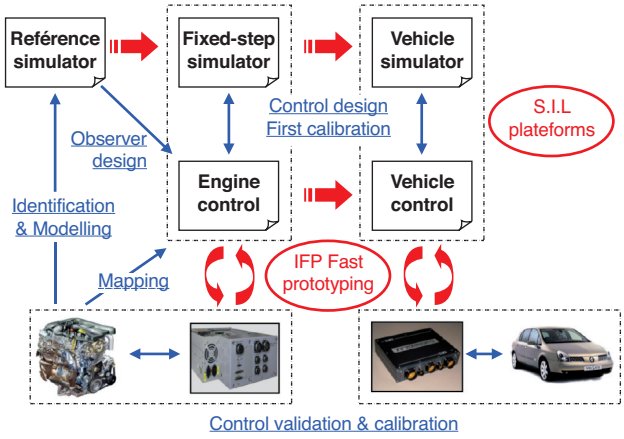

Figure 1

Simulation-based development process.

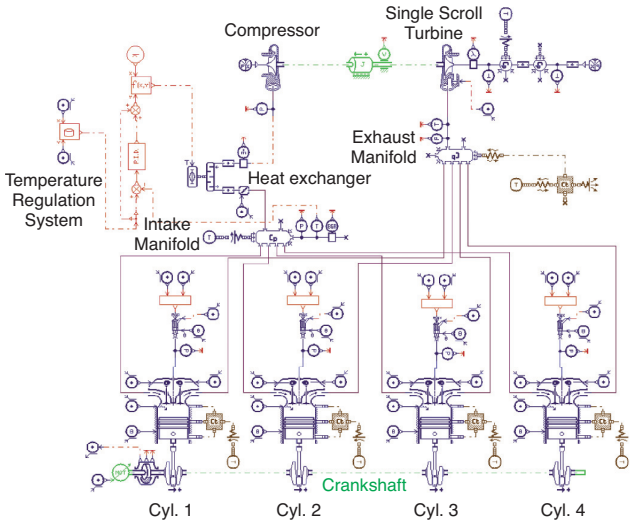

Figure 2

Turbocharged gasoline direct injection engine model.

IFP process used for engine control development is presented in Figure 1. Based on AMESim platform, a high frequency 0D engine simulator with a high representative capability has been set to better understand the phenomena involved on the process to control [3]. Observers and controllers design can be first achieved in continuous variable step simulation. To reduce computation time, a real time S.I.L. (Software In the Loop) platform based on reference engine simulator is used to finalize engine control design, before a complete validation and calibration on test bed with an IFP full-pass rapid prototyping system.

In the same way, a complete vehicle simulator has been set on real-time platform to design vehicle control. Then, validation and calibration have been done under road tests for performances and drivability, and New European Driving Cycle on vehicle bench for pollutant emissions.

1.2 Engine Simulator

To deal with the different SI engine control issue, a high frequency 0D engine simulator, presented in Figure 2, has been developed on the AMESim platform thanks to a specific engine library called IFP-ENGINE [4]. The simulator is representative of a turbocharged SI engine equipped with a direct injection system and a Variable Camshaft Timing (VCT) device. To be computed with a good accuracy, the simulator uses the variable time step continuous solver of the AMESim platform.

A complete description of the engine simulator and its different sub-models is presented in [5]. This simulator has notably the particularity to use the phenomenological combustion model CFM-1D based on a two-zone approach (fresh and burnt gases) [6].

The engine simulator is in a first time calibrated on a few steady states points to fill in all the unknown parameters. After this, the engine model is evaluated on complete steady state bench results to evaluate the relevance and the accuracy of the modelling and the calibration on the whole range of operating conditions. For all the tested operating points, the simulator results are then compared to test-bed. Comparisons are carried out on the whole values measured on test-bed: pressure and temperature on the whole air-path, mass flow rate, IMEP... Figure 3 shows the good agreement between the engine model and the real one concerning intake mass flow rate.

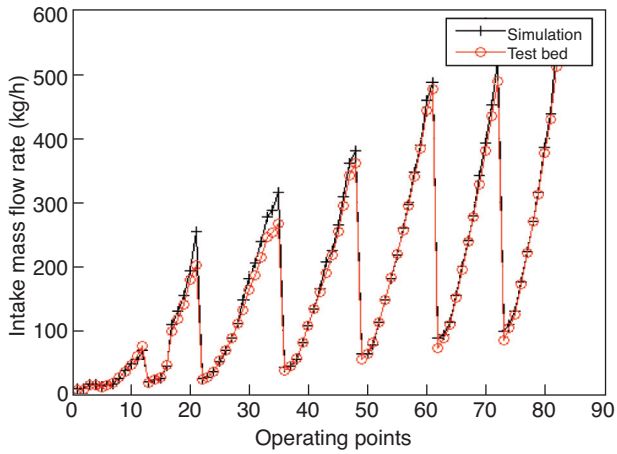

Figure 3

Model/experiment mean intake mass flow rate comparison.

Engine control design under transient conditions need fast computation time and the using of a fixed time step solver for real-time integration. These two constraints are not compatible for the moment with the phenomenological combustion model. The fixed step simulator uses thus an identified combustion model.

The identified combustion model generation process is based on neural network identification of cylinder pressures according to combustion conditions (manifold pressure, VCT positions, injection time, spark advance...). A campaign on a very large amount of operating conditions is realised to create a complete combustion data base. These data are then post-treated for the neural network learning, and the identified neural networks are finally integrated in the combustion model.

The fixed-step engine simulator is then tested under transient conditions to validate the simulator dynamic behaviour, particularly the turbocharger dynamic in terms of turbo-lag *(Fig. 4)*. The presented transient test is realised at 2000 rpm. The throttle and the waste gate are respectively fully opened and closed in order to validate the turbocharger dynamic behaviour without any parasitic effect due to the actuators. It shows the good agreement between the model and the real engine. The increase in manifold pressure is identical to the test bed results. This good behaviour can be also remarked on turbocharger speed during transient.

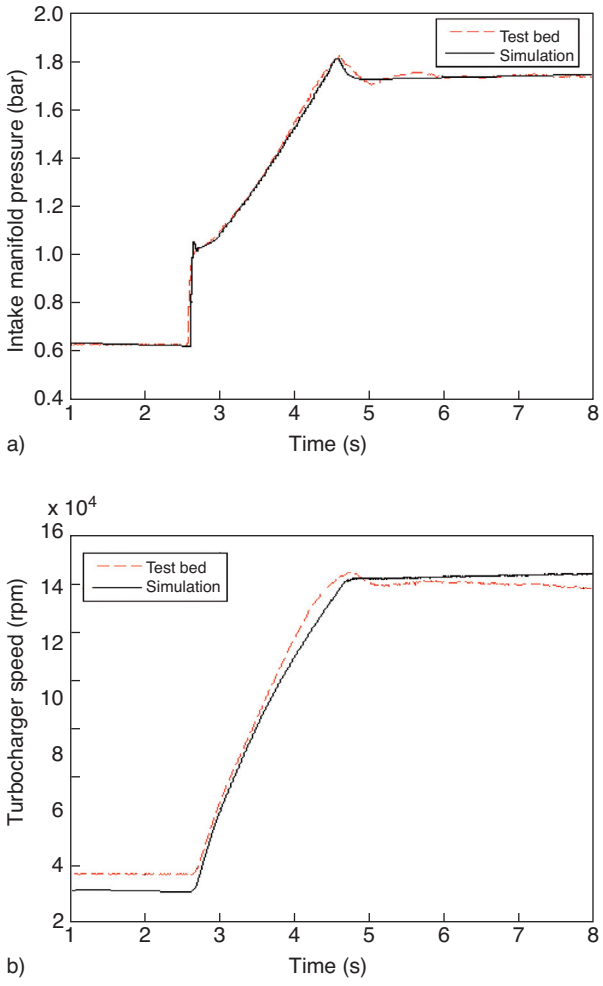

Figure 4

Model/experiment intake manifold pressure and turbocharger speed comparison during transient.

2. DOWNSIZED SI ENGINE CONTROL

The main issue of downsized SI engine control design is determination of relevant variables to control to reach performance, fuel consumption and pollutant emissions demands. Regarding engine technologies and phenomena understanding, in-cylinder gases masses (trapped air, burned gases and air scavenging) appears to be important variables to control. After definition of an adapted torque-structure, this section will focus on the main contribution: design of accurate observers and non-linear controllers for unmeasured in-cylinder gases masses.

2.1 In-Cylinder Gases Masses: A Control Issue

The torque is directly linked to the air mass trapped in the cylinder (from D_{cyl}) for a given engine speed. An efficient observation and control of the air mass trapped in the cylinder is required to obtain the desired torque.

The air intake of a turbocharged SI Engine, represented in Figure 5 can be described as follows. The compressor (pressure P_{int}) produces a flow going through the throttle into the intake manifold (pressure P_{man} and temperature T_{man}). The flow that gets into the cylinders D_{cyl} passes through the intake valves, whose timing is controlled by the intake Variable Camshaft Timing VCT_{in} actuator. After the combustion, the gases are expelled into the exhaust manifold through the exhaust valve, whose timing is controlled by the exhaust VCT_{exh} actuator. The exhaust flow is split in two parts: the turbine flow and the waste gate flow. The turbine flow powers up the turbine and drives the compressor through a shaft. Thus, the supercharged pressure P_{int} can be adjusted by the turbine flow which is controlled by the waste gate *WG*.

The effects of Variable Camshaft Timing (VCT), illustrated in Figure 6, can be summarized as follows.

On one hand *(Fig. 6a)*, when exhaust pressure is greater than manifold pressure during overlapping, a part of combustion products which would otherwise be expelled during the exhaust stroke are retained in the cylinder during the subsequent intake stroke. This dilution of the mixture in the

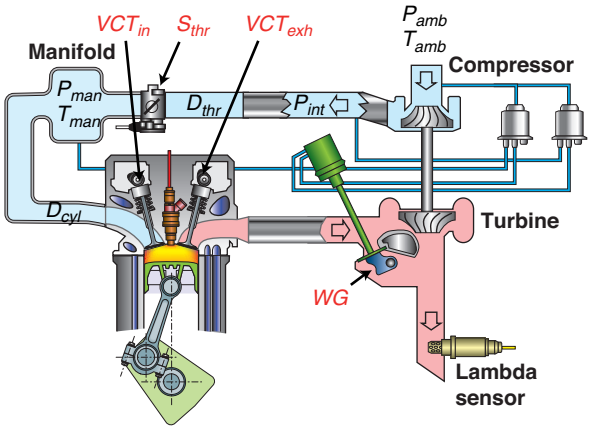

Figure 5

Air intake of a turbocharged SI engine with VCT.

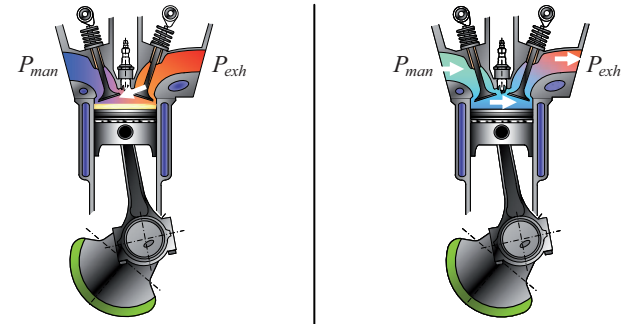

a. $P_{exh}>P_{man}$: Burned gases

b. $P_{man}>P_{exh}$: Scavenging

Figure 6

Recirculated Gases Mass (RGM).

cylinder reduces the combustion temperature and limits the NOx formation, but the combustion stability can be reduced too. Therefore, it is important to control an optimal value of burned gases in the cylinder.

On the other hand *(Fig. 6b)*, when exhaust pressure is greater than manifold pressure during overlapping, air scavenging appears. A part of air passes directly from the intake to the exhaust valve through the cylinder. In that case, the turbocharger and engine torque response times are decreased. Indeed, the flow which passes through the turbine is increased and the energy retrieved by the turbine is given to the compressor. In transient, it is very important to control this scavenging.

When there is scavenging from the intake to the exhaust, the burned gases are insignificant. Thus, only one variable, noted here RGM (Recirculated Gases Mass), is used to describe the scavenged air and burned gas masses:

$$RGM = \begin{cases} M_{burned\ gas} & \text{if } M_{burned\ gas} > M_{scavenged} \\ -M_{scavenged} & \text{else} \end{cases} \quad (1)$$

2.2 A Torque-Based Structure

The main goal of engine control is improvement of torque response, as far as possible in optimal ignition conditions, with an accurate AFR control. This leads to consider three main set points:

– The torque set point linked to the driver's request.
– AFR set point for an optimal exhaust catalytic conversion and fuel consumption.
– Torque efficiency set point for stability or pollutants consideration during idle or warm up strategies.

The proposed torque-based control structure of the downsized SI engine with VCT is presented in Figure 7. It shows the contribution for an innovative control: the in-cylinder gases masses are major variables leading not only air path control, but also fuel and ignition paths.

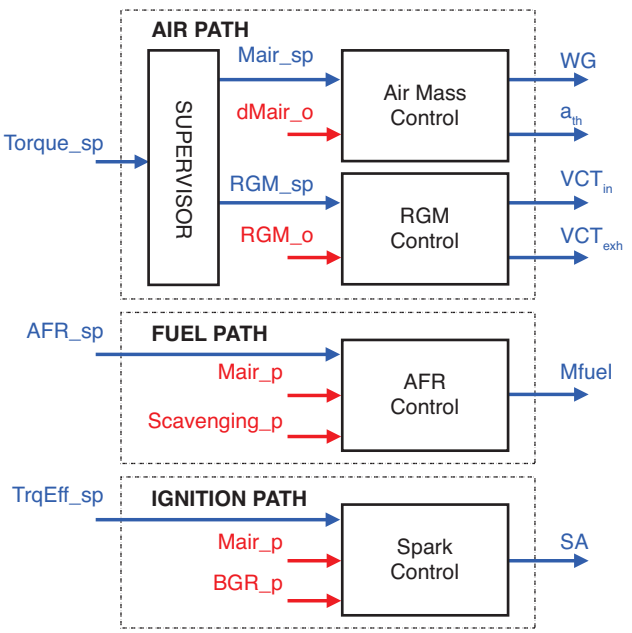

Figure 7

Proposed torque-based structure for downsized SI engine.

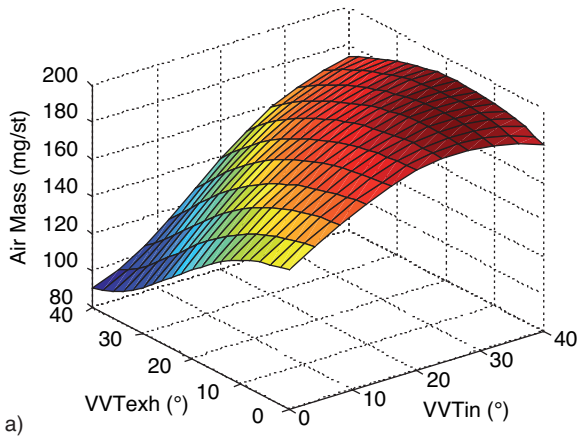

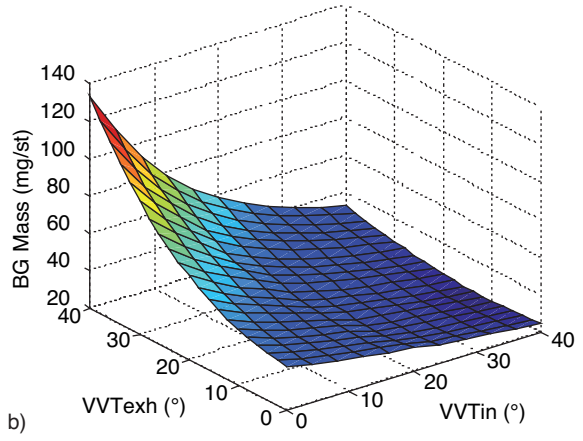

Figure 8

In cylinder air mass and recirculated gases mass at Ne = 2000 rpm and Pman = 0.4 bar.

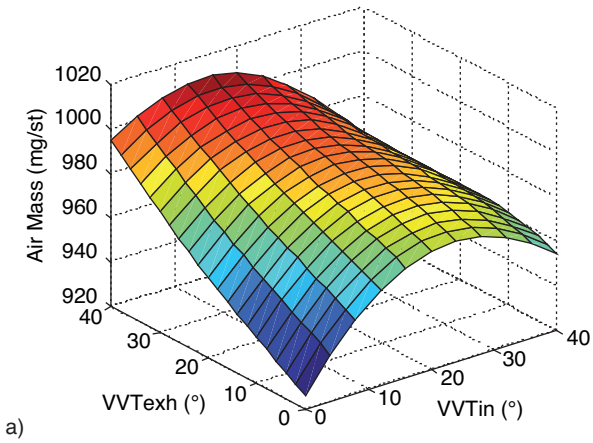

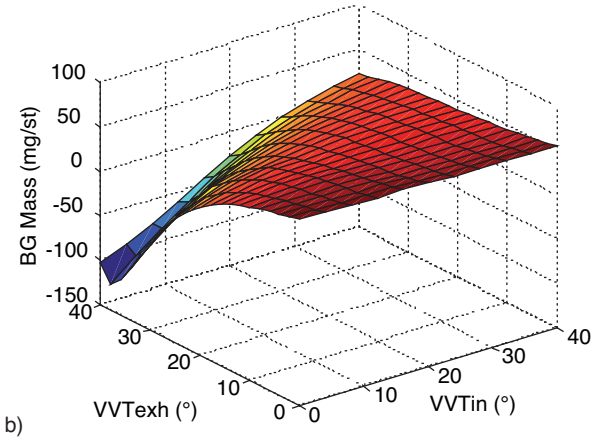

Figure 9

In cylinder air mass and recirculated gases mass at Ne = 2000 rpm and Pman = 2 bars.

From indicated torque set point, a supervisor computes the two main air path set points: trapped air mass *Mair_sp* and recirculated gases mass *RGM_sp*. Air path control is thus splitted into two parts: the air mass control and the recirculated gases mass control. A benefit of such a supervisor is to be able to manage transient trajectories independent from steady-state condition considering the engine ability to go from a point to another. Another one is the ability to generate different trajectories, in warm-up conditions for example, at a high level in control scheme.

The in-cylinder gases masses observation is also a main issue for fuel and ignition path. In order to get an accurate AFR control even in transient, an accurate observation, and even prediction, of trapped and scavenged air masses is necessary to compute feed forward fuel mass command. In order to keep optimal ignition conditions (optimal torque for a lowest fuel consumption), particularly during transient, spark angle control is based on in cylinder air mass and burned gases estimation.

2.3 In-Cylinder Gases Masses Observer

2.3.1 Observer Issues

An efficient observation of air mass trapped in cylinder and recirculated gases mass is a crucial issue of downsized SI engine control with VCT.

Air mass trapped each stroke in cylinder can be described from volumetric efficiency [7]:

$$Mair_{cyl} = \frac{\eta_{vol} . V_{cyl} . P_{amb}}{R T_{man}} \quad (2)$$

η_{vol} Volumetric efficiency
V_{cyl} Cylinder volume
P_{amb} Atmospheric pressure
T_{man} Intake manifold temperature

Without VCT and in steady-state conditions, volumetric efficiency depends only of engine speed and intake manifold pressure. Different valve timing overlaps change the exhaust manifold pressure and the recirculated gases mass, and thus volumetric efficiency. So, VCT positions have to be taken into account and it would need a large amount of test to cover a wide range of operating conditions, even with a design of experiment methodology.

A preferred methodology is to design a model-based observer closed-loop on air flow rate measurement. In order to speed up convergence, a feed forward quasi-static neural model taking in account VCT positions is used. This model is learnt from high-frequency 0D engine simulator.

Moreover, a recirculated gases mass model is needed and studying burned gases and scavenging on test bed is complex because it can't be directly measured. A quasi-static neural model taking in account VCT positions is also learnt from high-frequency 0D engine simulator.

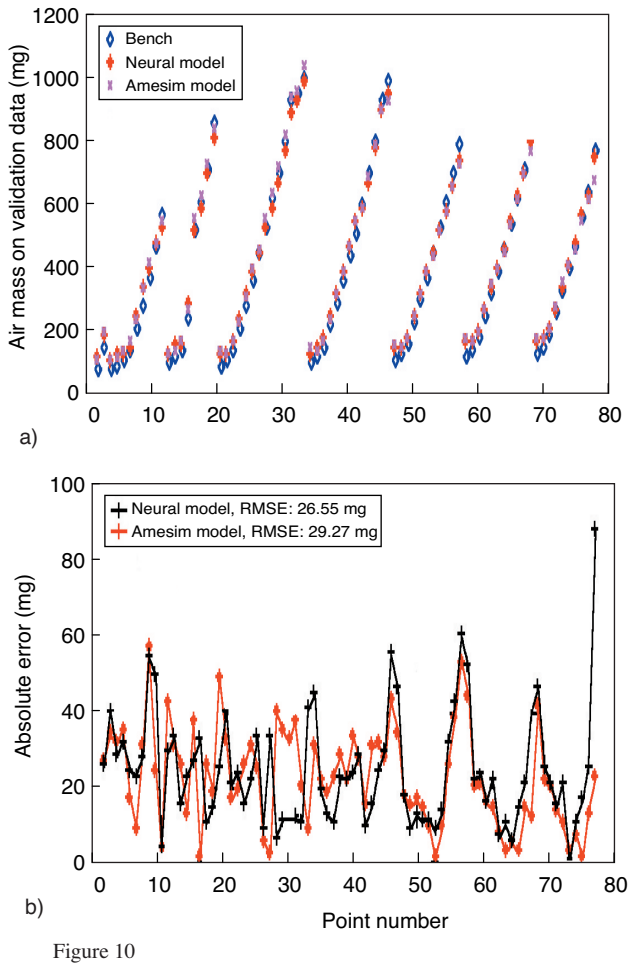

Figure 10

In-cylinder air mass neural model and engine results comparison on validation base.

2.3.2 Quasi-Static Neural Models

A preferred methodology is thus to build models from high-frequency 0D engine simulator. As this physical model is too complex to be directly embedded, black-box solution as neural networks become an attractive technique for this purpose. Indeed, a broad range of neural network architectures can be found for system modeling and identification, particularly for global static nonlinear models [8]. Then, an exhaustive learning process can be achieved. The learning base (about 6800 points) comprises all the representative static operating points: manifold pressure from 0.3 to 2.4 bars, engine speed from 750 to 5500 rpm, and intake and exhaust valve timing overlap on a 40 crankshaft angle range. Both air mass trapped in cylinder and recirculated gases mass static neural model are computed:

$$\hat{M}air_{cyl} = \frac{V_{cyl}.P_{amb}}{R.T_{man}} f_{nn}(P_{man}, N_e, VCT_{in}, VCT_{exh}) \quad (3)$$

$$\hat{RGM} = f_{nn}(P_{man}, N_e, VCT_{in}, VCT_{exh}) \quad (4)$$

Figures 8 and 9 show neural models behavior to VCT variations while fixing engine speed and manifold pressure.

Neural network models are validated on a different base (about 80 points) covering all optimal operating points of engine mapping (engine speed, IMEP) on test bed.

Figure 10 compare directly air mass neural model to engine simulator and test bed results. It shows that this methodology gives quite good results and than most of errors come from engine simulator bias. Figure 11 shows a good correlation between recirculated gases mass neural model and engine simulator. It can't be compared to real engine results because of no measurement. But the work done on residual burned gases estimation in engine simulator [5] assumes a good representative capability.

2.3.3 Trapped Air Mass Closed-Loop Observation

A final objective is to design a closed-loop observation to avoid bias estimation. The air flow rate measurement between compressor and throttle, and feed-forward neural observations of trapped air flow and scavenged air flow are used in intake pressure equation to closed-loop the observation. To avoid noise on air flow measurement, a Kalman filter is used.

Differentiating the ideal gas law while considering a constant intake temperature (or slow variations), gives:

$$\dot{P}_{man} = \frac{R.T_{man}.(D_{thr} - \hat{D}_{cyl} - \Delta D_{cyl} - \hat{D}_{scavenged})}{V_{man}} \quad (5)$$

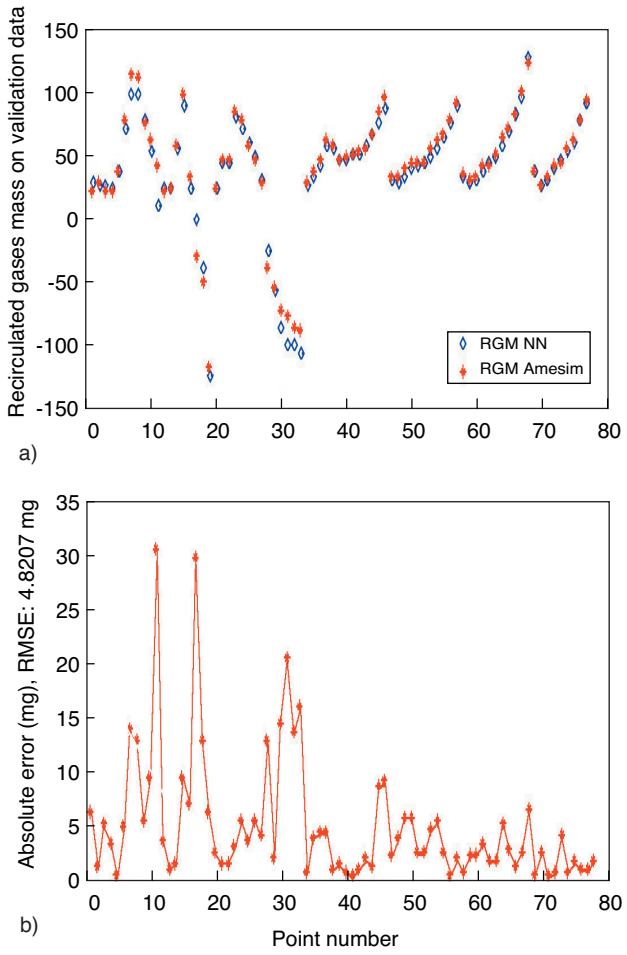

Figure 11

Recirculated gases mass neural model and AMEsim simulator results comparison on validation base.

D_{thr} Flow through the throttle (in the manifold)
$\hat{D}_{cyl}$ Neural observation of air flow trapped
$\hat{D}_{scavenged}$ Neural observation of scavenged air flow
$\Delta\hat{D}_{cyl}$ Feedforward error estimation

D_{thr} is measured with air flow rate sensor between compressor and throttle.

Considering a slow air flow error variation, a continuous state representation is set from this equation:

$$\begin{cases} \dot{X} = AX + BU \\ Y = CX \end{cases} \quad with\ X = \begin{pmatrix} P_{man} \\ \Delta D_{cyl} \end{pmatrix}\ U = \begin{pmatrix} D_{thr} \\ \hat{D}_{cyl} \\ \hat{D}_{scavenged} \end{pmatrix} \tag{6}$$

After discretization, the kalman filter representation consists in adding measurement and state noises:

$$\begin{cases} X_k = A_d X_k + B_d U_k + w_k \\ Y_k = CX_k + v_k \end{cases} \quad with \quad \begin{matrix} A_d = AT_e + I \\ B_d = BT_e \end{matrix} \tag{7}$$

T_e Sample time

Thus Kalman filter equations are:

$$\begin{aligned} &\hat{X}_{k+1/k} = A_d\hat{X}_{k/k-1} + B_dU_k + K_k\left(Y_k - C\hat{X}_{k/k-1}\right) \\ &with: \\ &K_k = A_dP_{k/k-1}C^T\left(CP_{k/k-1}C^T + V\right)^{-1} \\ &P_{k+1/k} = A_dP_{k/k-1}A_d^T + W - K_kC_dP_{k/k-1}A_d^T \end{aligned} \tag{8}$$

K_k Kalman Filter gain
W Measurement noise covariance matrix
V State noise covariance matrix

Quasi-static neural models and Kalman filter are executed on line each TDC. The state ΔD_{cyl} is thus integrated to provide air mass error:

$$\Delta M_{air} = \Delta D_{cyl} \cdot \frac{120}{N_e\, n_{cyl}} \tag{9}$$

N_e Engine speed (rpm)
n_{cyl} Number of cylinders

Measurement and state noise covariance matrix have been identified in simulation, looped on high frequency 0D engine model, for a best stability and convergence. Figure 12 shows final results of Kalman filter closed-loop on engine test bed after a final tune. During this test, an offset was applied on neural model in order to voluntary increase the estimation bias and see the closed-loop efficiency. It clearly shows its interest. Using air flow rate measurement eliminates model static bias without adding measurement noise or pumping during transients (*i.e.* at 29 s and at 40.5 s) on air mass trapped observation.

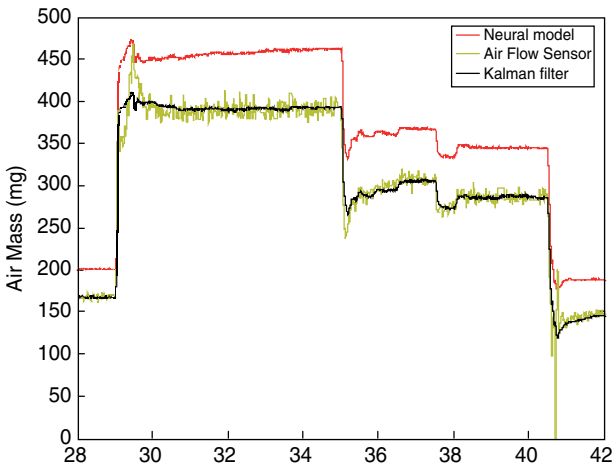

Figure 12

In-cylinder trapped air mass closed-loop observation results on engine test bed.

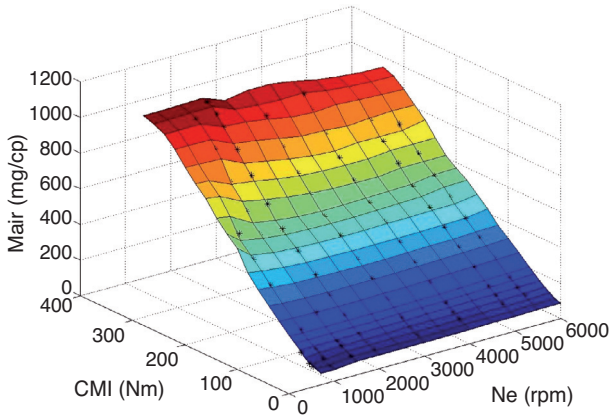

Figure 13

Air mass set point function of engine speed and torque set point.

2.4 Air Mass Control

The torque is linked to the air mass trapped in the cylinder for a given engine speed. In air path supervisor, air mass set point comes from a 2D look-up table depending of indicated torque set point and engine speed *(Fig. 13)*.

As presented in Figure 14, the air mass control commands the throttle and waste gate opening. In order to keep standard structure, actuators control is based on intake manifold pressure. Then it is necessary to compute from the air mass set point a manifold pressure set point leading air actuators closed loop controls.

2.4.1 From Air Mass to Manifold Pressure

In a SI engine with Variable Camshaft Timing, there is no one-to-one correspondence between the air mass trapped and the intake manifold pressure at fixed engine speed. It is thus necessary to model the intake manifold pressure function of VCT positions. A preferred methodology is thus to learn quasi-static neural model from 0D engine simulator as for in-cylinder gases masses observers:

$$P_{man} = f_{nn}(M_{air}, N_e, VCT_{in}, VCT_{exh}) \quad \text{with } T_{man} = T_{amb} \tag{10}$$

Quasi-static neural models learnt from 0D engine simulator got bias comparing to engine. Consequently, intake manifold pressure model also learnt static errors from 0D engine simulator, impacting correspondence between manifold pressure and air mass.

A kalman filter is used to closed-loop air mass observation and estimate static bias from air flow measurement. Considering that the intake manifold pressure neural model is an inversion of trapped air mass neural model, a proposed solution is thus the subtraction of trapped air mass error estimation *(Equation 9)* to air mass set point as input of intake manifold pressure model. Manifold temperature influence is taken in account on air mass input considering (2), and intake manifold pressure set point computation is thus given by:

$$P_{man\,sp} = f_{nn}\left(\frac{T_{man}}{T_{amb}}(M_{air\,sp} - \Delta\hat{M}_{air}), N_e, VCT_{in}, VCT_{exh}\right) \tag{11}$$

Figures 21 and 23 show that using bias estimation to correct intake manifold pressure set point gives good results. Trapped air mass observation and consequently indicated torque measurement, follow set point trajectory without static error.

2.4.2 Intake Throttle Control

A proposed structure is based on a classical model-based feedforward control *(Fig. 15)*. The controlled variable is the intake manifold pressure P_{man} and the manipulated variable is the intake throttle area S_{thr}. It used an identified intake manifold model with a physical throttle restriction model (Barré Saint-Venant).

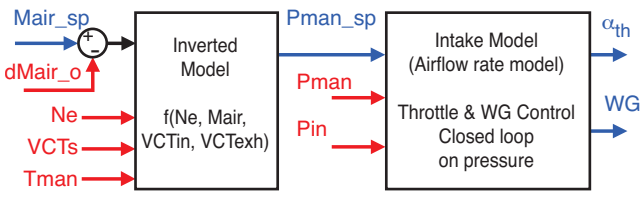

Figure 14

Proposed scheme for air mass control.

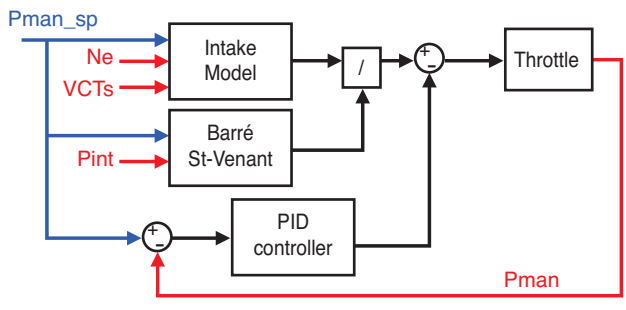

Figure 15

Intake throttle control scheme.

From Equation 5, considering steady-state condition, the flow through the throttle (D_{cyl}) is equal to the flow through the intake valve (D_{in}):

$$D_{thr} = D_{in} = D_{cyl} + D_{scavenged} \tag{12}$$

On one hand, the flow through the throttle is calculated by the Barré Saint-Venant equation based on upstream and downstream pressures ratio:

$$D_{thr} = S_{thr} P_{\text{int}} f(T_{man}, P_{man} / P_{\text{int}})$$
$$with: f(T, P_r) = \sqrt{\frac{2\gamma}{(\gamma - 1)RT}\left(P_r^{\frac{2}{\gamma}} - P_r^{\frac{\gamma+1}{\gamma}}\right)} \tag{13}$$

P_{int} Intercooler (upstream throttle) pressure
P_{man} Intake manifold (downstream throttle) pressure
T_{man} Intake manifold temperature
γ Ratio of specific heats of air

On the other hand, the flow through the intake valve D_{in} is calculated from air and recirculated gases masses quasi-static neural models *(Equations 3, 4)* using intake manifold pressure set point as input. To reduce static error, the air mass model bias estimation coming from Kalman filter closed loop is added *(Equation 9)*:

$$D_{in} = \frac{n_{cyl} N_e}{120}\left(\hat{M}air_{cyl} + \hat{M}air_{scavenged} + \Delta Mair\right) \tag{14}$$

Consequently (12), (13) and (14) give feedforward throttle area S_{thr}. To avoid static error and reach air mass set points, intake manifold pressure control is completed with a classical PID controller on measurement.

Engine test bench results in Figure 16 give quite good results on pressure control. It shows that feedforward term is predominant and more accurate intake manifold model is, better the control is.

2.4.3 Waste Gate Control

A proposed structure is based on a classical feed forward control *(Fig. 17)* manipulating waste gate command. The controlled variable is the supercharging pressure P_{int}. It assumes that close to pressure set point, the throttle will stay fully opened ($P_{int} > P_{man}$). Waste gate control issue is a fast rise in pressure while limiting overshoot.A waste gate look-up table function of engine speed and manifold pressure is used as feed forward action *(Fig. 18)*. It corresponds to steady-state waste gate commands as defined by engine mapping on overall (Engine speed, IMEP) points. This ensures an inversion of the characteristic of the turbocompressor, and thus a linearization of the system.

In order to reach set point taking advantage of this linearization, a PI controller acts on the manifold pressure set point in input of waste gate characteristic. This controller can thus be adjusted to stabilize the system with one uniform adjustment on the operating range.

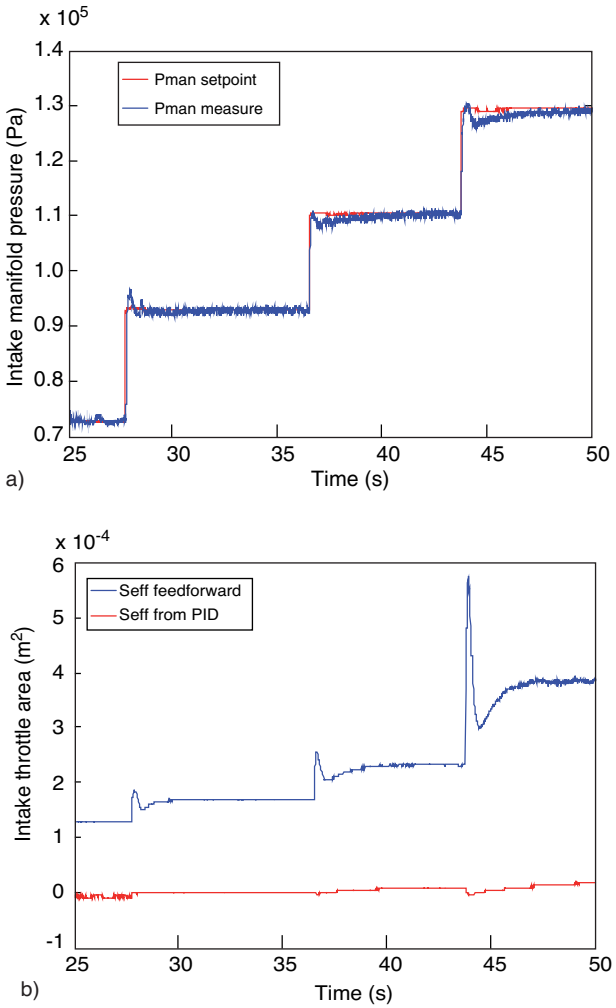

Figure 16

Intake manifold pressure control results.

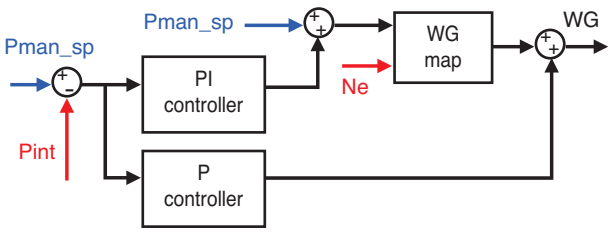

Figure 17

Wastegate control scheme.

In order to speed up pressure rising during strong torque request variation, a second P term controller fully closes the waste gate in transient.

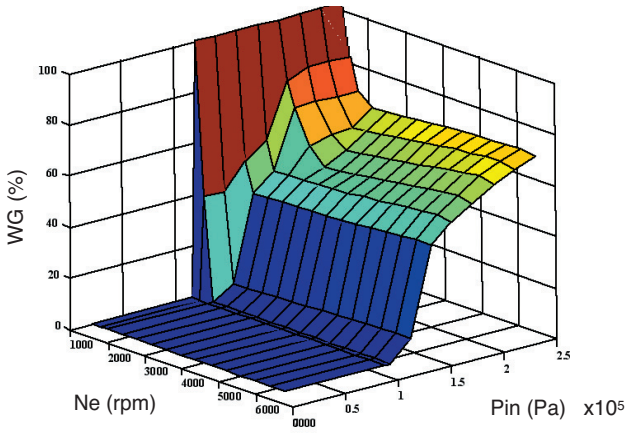

Figure 18

Feedforward wastegate command.

Results on 50 to 250 Nm torque transient are presented in Figure 19. It shows how throttle first fully open and waste gate fully close to reach target. Because of compressor inertia, there is a supercharging pressure over lap controlled by throttle closing in order to keep intake manifold pressure on target. Supercharging pressure is then controlled to reach target while keeping throttle full opened.

2.5 Recirculated Gases Mass Control

A good control of residual burned gases at low load is important to minimize fuel consumption and pollutant emissions. Scavenging at high load can improve combustion efficiency. RGM control issue is thus the independence with air mass control and the ability to reach different set points while keeping air mass constant.

2.5.1 RGM Supervision

Tests in simulation on real-time engine simulator shows there is an infinite solution area for VCTs positions to reach air mass and recirculated gases mass set points. For a given (Mair, RGM) target, solutions are a line:

$$VCT_{exh} = a.VCT_{in} + b \quad (15)$$

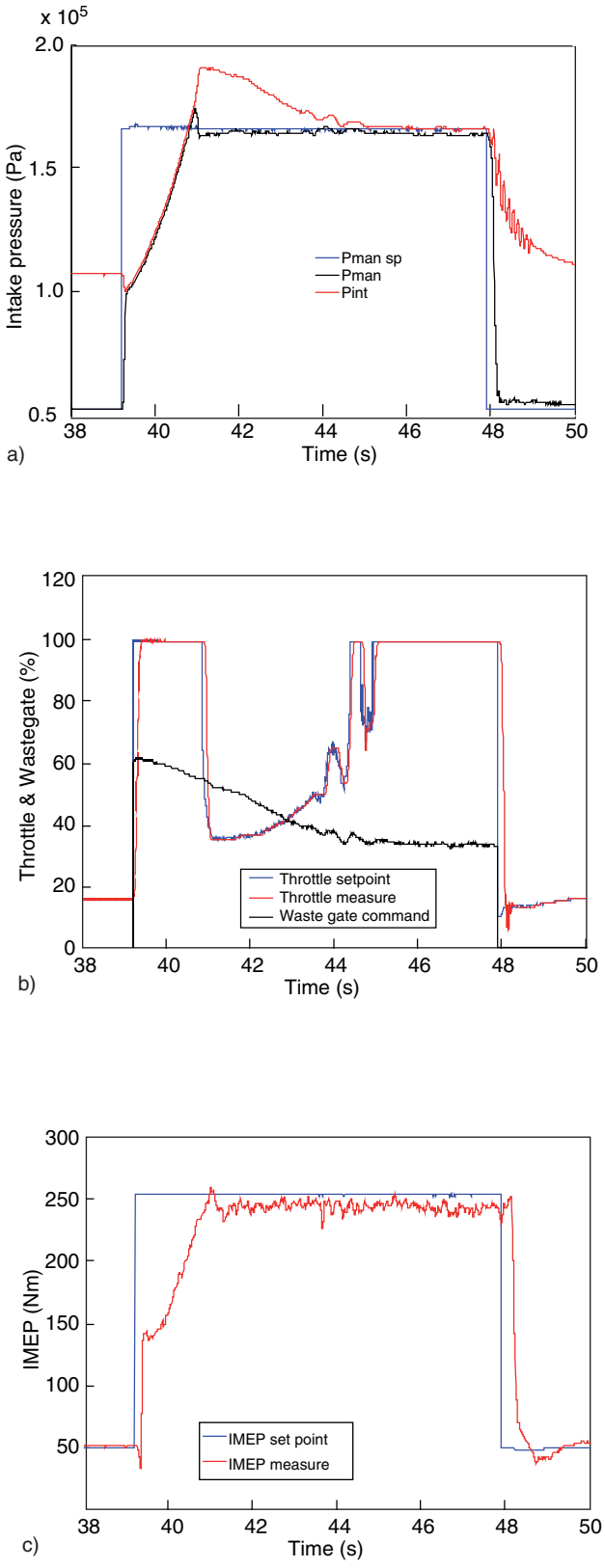

Figure 19

Transient results at 2000 rpm engine speed.

RGM Control must thus been supervised to reach one:

– Optimization algorithm reaches nearest solution without constraints, but this solution may not be optimal in term of pollutants and fuel consumption.
– One VCT position is constraint.
– One optimal solution is known and algorithm converges to this point.

During engine mapping on test bed, optimal VCT positions have been found for each (Engine speed, IMEP) operating point. It gives in warm conditions:

$$\begin{aligned} VCT_{in\ opti} &= f(N_e, M_{air}) \\ VCT_{exh\ opti} &= f(N_e, M_{air}) \\ RGM_{sp} &= f_{nn}(P_{man\ sp}, N_e, VCT_{in\ opti}, VCT_{exh\ opti}) \end{aligned} \quad (16)$$

Figure 20 shows results of those optimal VCT setting on recirculated gases mass set point.

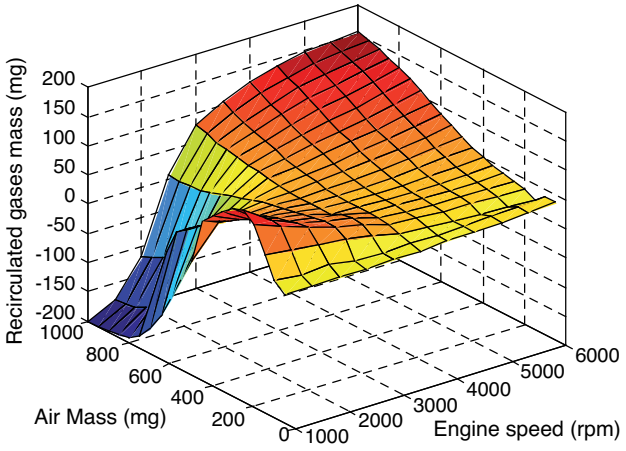

Figure 20

Optimal recirculated gases mass set point function of engine speed and air mass set point in warm conditions.

Considering stability, pollutant emissions and fuel consumption, optimal recirculated gases mass is different during warm up than in warm conditions. Thus supervision has to take in account temperature to reach a different trajectory, for example fixing warm optimal VCT_{exh} position while limiting overlap or just limiting burnt gases. Section 3.2 explains how RGM supervision is used on vehicle to reach pollutant constraints on NEDC cycle.

2.5.2 Optimization Control

The controlled variable is the estimated variable RGM, coming from static neural model, the controlled variables are intake and exhaust variable camshaft timing.

Thus, the burned gases control consists in a non-linear optimization method based on RGM neural model. The goal is a real time minimization of next criteria:

$$J = (\hat{RGM} - RGM_{sp})^2 + \rho_1 \Delta VCT_{in} + \rho_2 \Delta VCT_{exh} \quad (17)$$

RGM Recirculated gases mass observation
RGM_{sp} Recirculated gases mass set point
ΔVCT_{in} Intake camshaft timing variation
ΔVCT_{exh} Exhaust camshaft timing variation
ρ_1, ρ_2 Weighting factors

The chosen method is a full-Newton Levenberg-Marquardt method [9]. The advantage is the convergence and the computational aspect for small order systems. The minimization algorithm [10] has been integrated in real time and solved with 2 iterations because of computational load aspect.

A validation test *(Fig. 21)*, starts from a chosen steady-state point, engine speed 2000 rpm and an indicated torque set point of 40 Nm. Air mass control reaches corresponding pressure and air mass while optimal RGM set point defines VCT positions. From this point, burnt gases mass is changed manually. Optimization control then follows defined trajectory and changes VCT positions in order to reach observation on set point accurately.

A main issue is to keep air mass constant while varying burnt gases in cylinder. As described in Section 2.3.1, correspondence between the air mass trapped in cylinder and the intake manifold pressure depends on VCT positions. Those results show how pressure neural model takes in account VCT variations to adapt intake pressure set point and keep air mass constant. Particularly, it confirms that the use of Kalman filter in order to estimate air mass observation bias helps to eliminate static error between air mass set point and measure.

2.6 AFR Control

AFR control issue is to keep fuel/air equivalent ratio constant in exhaust manifold for an optimal exhaust catalytic conversion in steady-state and transient. The methodology is to compute feed-forward fuel mass from trapped air mass estimation, taking into account of scavenging phenomenon.

2.6.1 Feed-Forward Fuel Mass Control

When scavenging is present, equivalent ratio is higher in cylinder than in exhaust manifold. Feedforward fuel mass computed from trapped air mass estimation will then cause a lean exhaust ratio. Scavenged air mass estimation is thus

used to compute a cylinder equivalent ratio set point corrected by scavenged air rate:

$$M_{fuel} = \left(EqRatio_{sp} + \frac{M_{scavenged}}{M_{air}} \right) . \frac{M_{air}}{PCO} + dM_{fuel} \qquad (18)$$

M_{fuel} Injected fuel mass estimation
dM_{fuel} Closed-loop fuel mass correction
$EqRatio_{sp}$ Fuel/air equivalent ratio set point
$M_{scavenged}$ Scavenged air mass prediction
M_{air} Trapped air mass prediction
PCO Stoichiometric air fuel ratio

A PI controller closed-loop on exhaust equivalent ratio measurement eliminates static errors in order to accuracy reach set point.

Fuel mass is computed each TDC and corresponding injector command is applied two TDC later (because of engine timing and hardware behaviour). In transient, trapped air mass is not corresponding anymore to observation during fuel mass computation. It causes important under or overshoot. To reduce this effect and keep equivalent ratio as constant as possible in transient, it necessary to get a trapped air mass prediction with a two TDC horizon.

2.6.2 Air Mass Prediction

As presented in Figure 22, a model-based prediction is achieved from intake manifold equation *(cf. Equation 5)*.

Predicted flow through throttle is computed according to Barré St-Venant equation *(Equation 13)* using as inputs throttle position set point and looped predicted manifold pressure. Predicted flow through intake valve is computed from air mass neural model *(Equation 3)* using as inputs variable camshaft timing set point and looped predicted manifold pressure. Manifold equation is thus integrated to provide predicted manifold pressure.

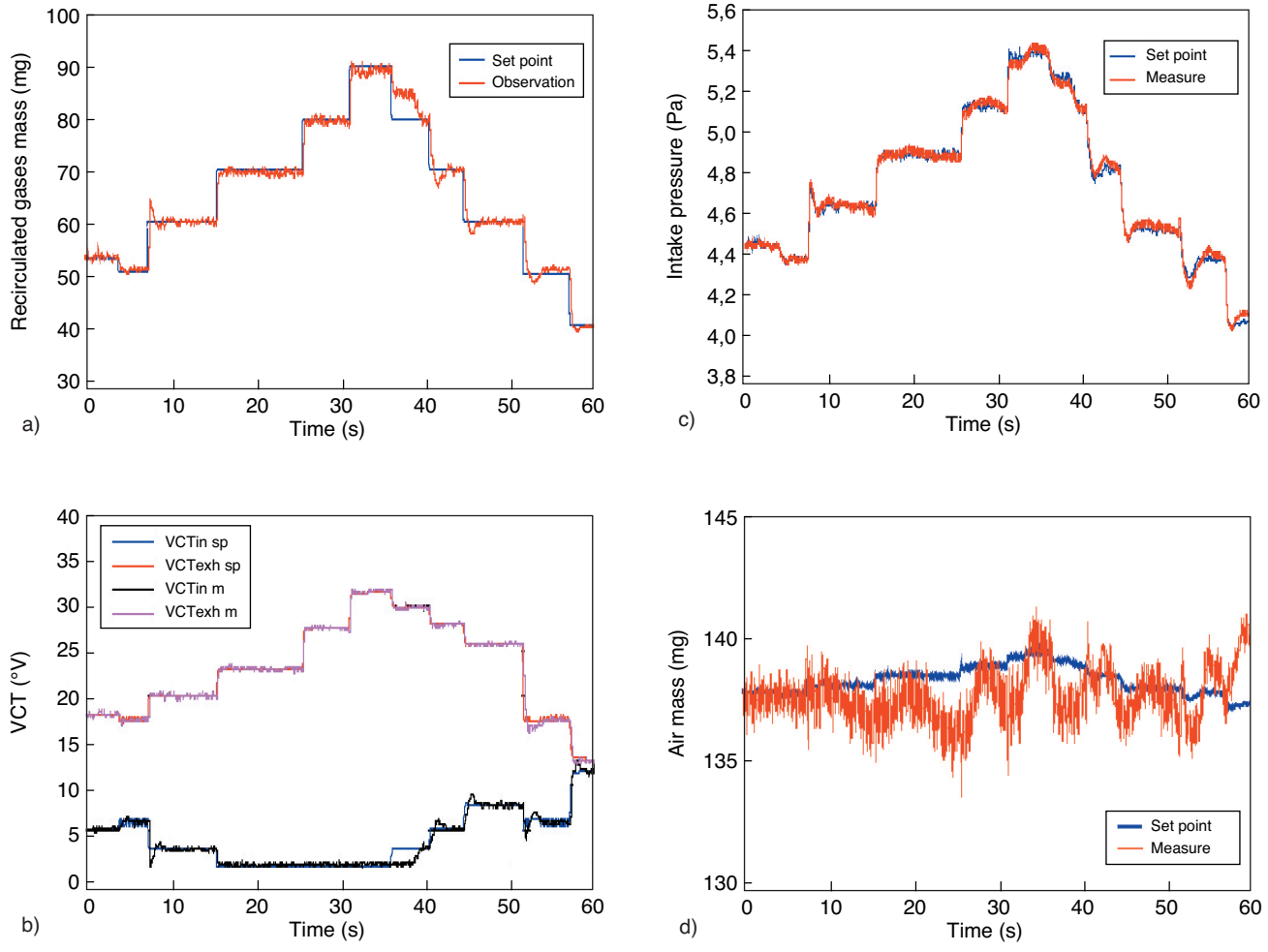

Figure 21

Recirculated gases mass variation on steady-state point: engine speed = 2000 rpm and indicated torque = 40 Nm.

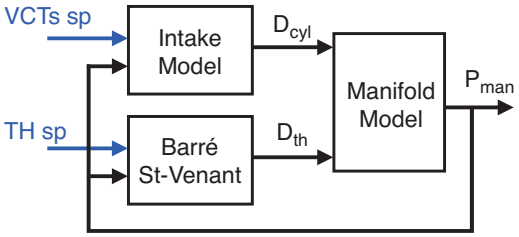

Figure 22

Pressure prediction scheme.

First order filters are tuned to take in account air actuators dynamics. To avoid static error, prediction is closed-loop on intake manifold measurement with a PI controller.

Figure 23 presents Fuel/air equivalent ratio control results on vehicle. With a simple air mass observation, there would be ratio undershoot during rising transient. We can thus see the effect of prediction: no significant undershoot and even overshoot due to prediction horizon.

3 VEHICLE INTEGRATION

3.1 Vehicle Layer: A Torque Supervision

Engine control is based on three main set points: indicated torque, Equivalence ratio, and torque efficiency. This section explains how those set points are managed on vehicle considering engine state (stop, start-up, idle, pedal, cut off...) determined function of engine speed and driver request.

Those states provide an effective torque set point. A friction model identified from engine mapping and function of engine speed, intake manifold pressure and coolant temperature estimate friction torque. Added to effective torque, it provides indicated torque set point to engine control layer.

STOP state

This state cuts injection (Equivalent ratio set point equal to zero) before start-up or during speed limiter.

START-UP state

The three main set points are determined function of engine speed and temperature:

$$\begin{aligned} Torque_{startup} &= f(N_e, T_{cool}) \\ TrqEff_{startup} &= f(N_e, T_{cool}) \\ EqRatio_{startup} &= f(N_e, T_{cool}) \end{aligned} \quad (19)$$

The advantage of this methodology is that calibration is quite simple and intuitive in order to quickly get functional starting, there is no direct actuation.

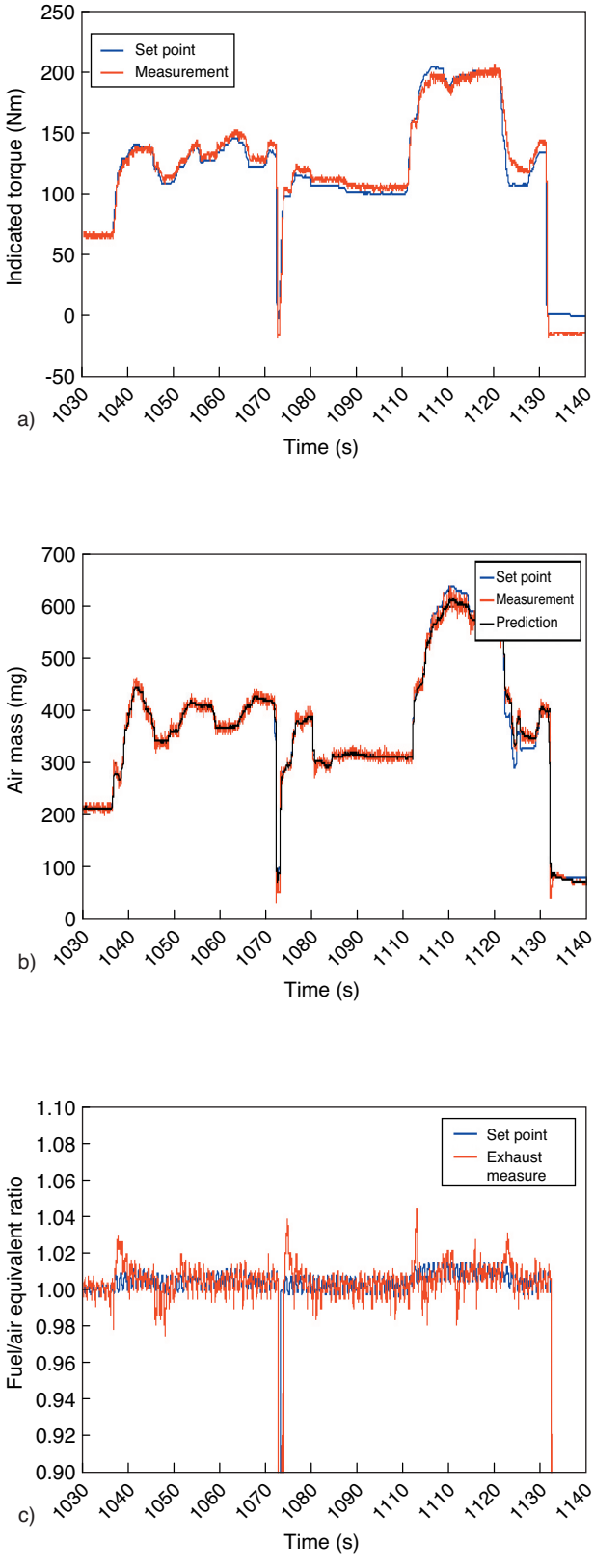

Figure 23

Fuel/air equivalent ratio control on vehicle.

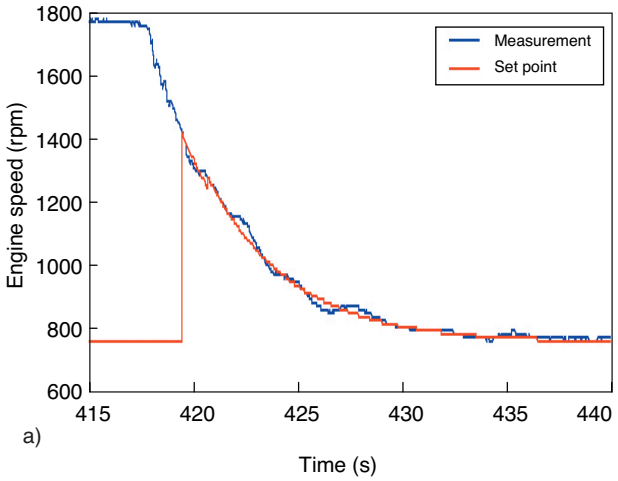

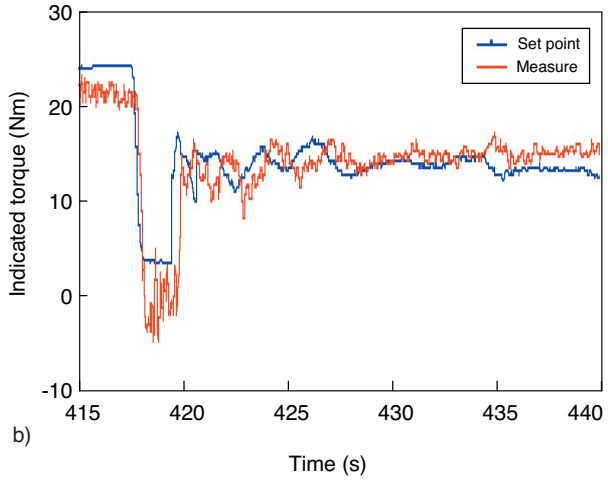

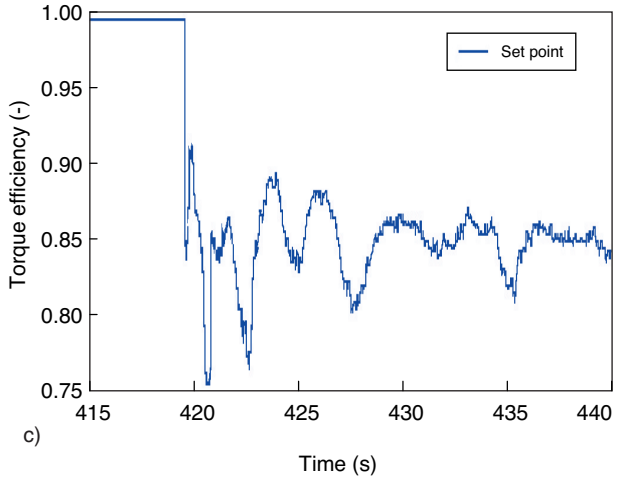

Figure 24

LQ controller for idle speed control results on vehicle.

IDLE state

Idle speed regulation is made with two main actions: a "slow torque" control from throttle (*i.e.* effective torque set point) and a "fast torque" control from spark advance (*i.e.* torque efficiency set point). A LQ controller has been synthesized in simulation closed loop on real-time vehicle simulator. A main issue for drivability is controller initialization. Init torque set point is function of previous state, engine speed and gear engaged. Another driveability issue is the way engine speed reach set point from entering threshold. A filter initialized to engine speed measurement able to control this dynamic function of gear engaged. LQ idle controller results are presented in Figure 24.

PEDAL state

This state takes in account driver acceleration request. Function of engine speed and driver request, a 2D look-up table provides effective torque set point *(Fig. 25)*.

In warm conditions, effective torque and equivalent ratio set point are set to one. As explain in next section, warm-up strategies can adapt those set points in order to reduce pollutant emissions.

CUT-OFF State

On pedal up detection, effective torque set point is filtered from previous request to negative torque set point function of gear engaged. The fuel/air equivalent ratio is thus set to zero in order to cut injection.

This vehicle layer has been first developed and validated on Hardware-In-the-Loop system using real-time vehicle model described in previous section. The torque-based approach, separating engine control development on engine test bed and vehicle requirements integration, makes it possible to obtain

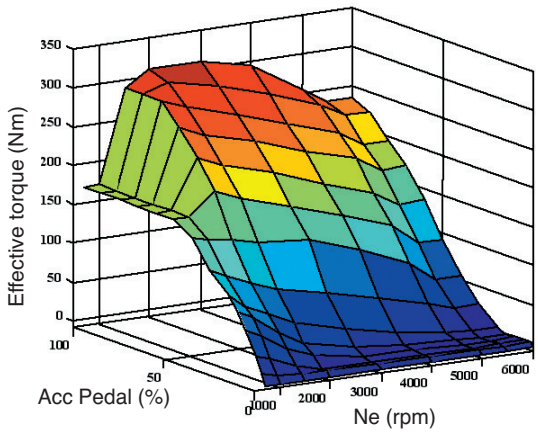

Figure 25

Effective torque set point cartography from driver request.

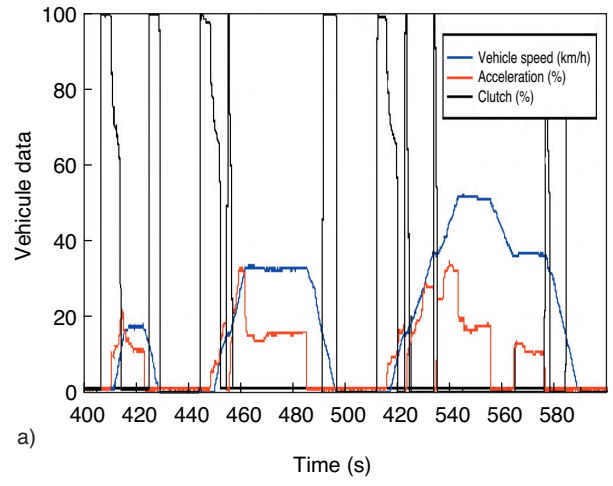

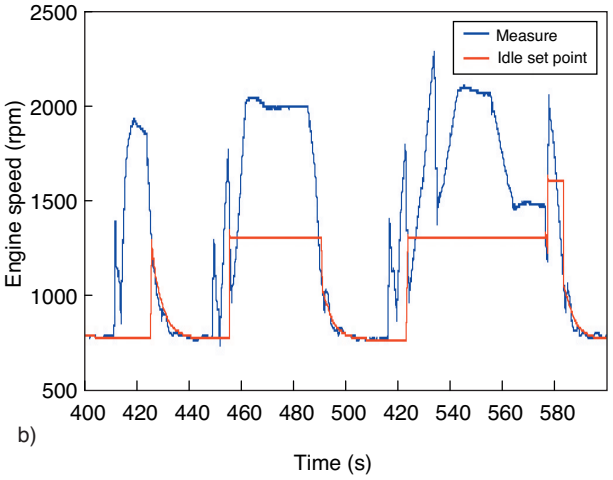

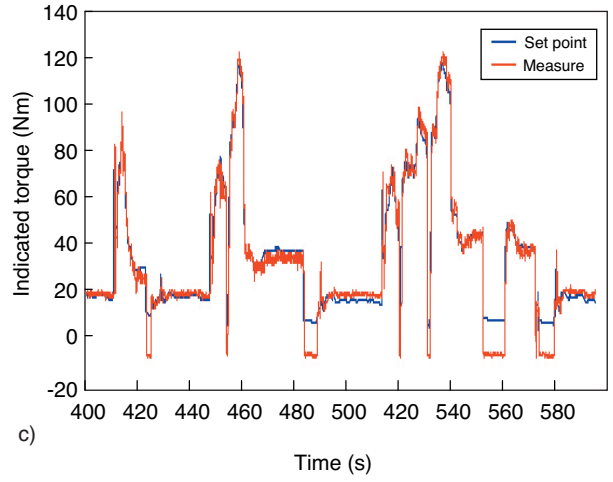

Figure 26

Torque-based engine control results on vehicle during ECE cycle.

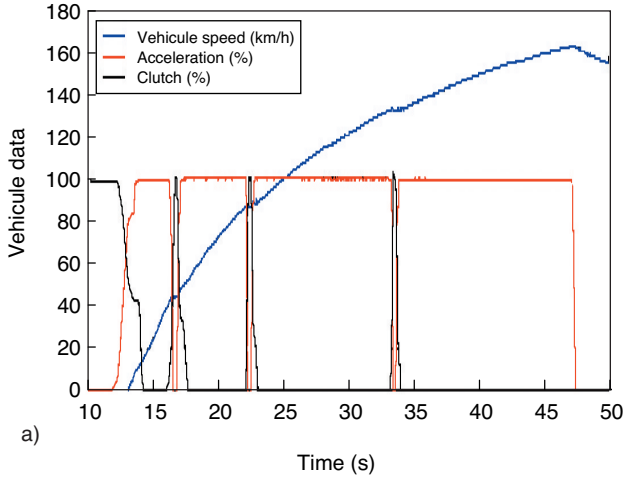

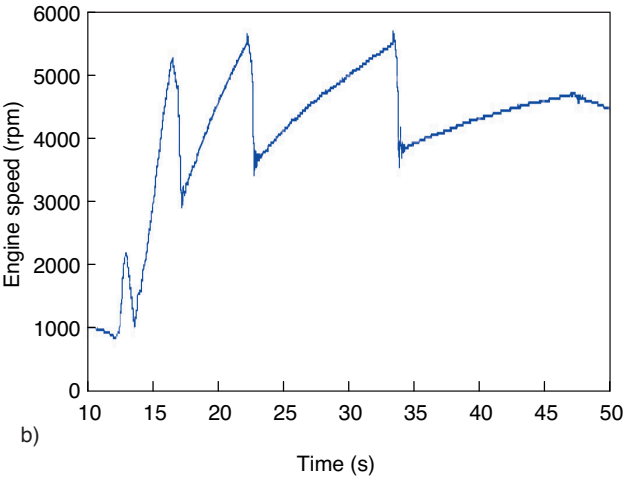

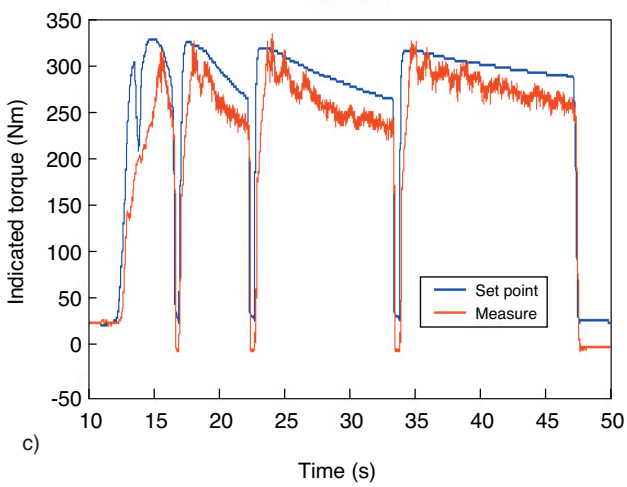

Figure 27

Torque-based engine control results on vehicle during launched kilometre test.

quickly and relatively easily a driveable demonstration car. It also facilitates final calibration in order to reach driveability and performance objectives.

Figure 26 presents engine control results during ECE cycle on rolling test bed. It shows a good global behaviour, with an accurate torque control. Some improvements are still possible, in particular during the pull-away phase. It could be achieved with a load torque observation.

Figure 27 presents engine control results during launched kilometre test on road test. Torque control is not so accurate because of impossibility to achieve steady-state validation at full load on rolling test bed. There are thus still static errors due to air flow rate sensor characteristic.

3.2 NEDC Strategies and Calibration

In order to validate IFP downsizing approach, in addition of drivability and performance objectives. A main issue of this demonstration car was to evaluate fuel consumption (*i.e.* CO_2 emissions) and pollutant emissions.

CO_2 emissions

Next table shows maximum torque and CO_2 emissions on NEDC of different reference engines. The goal of downsizing IFP engine was to reach performance of an equivalent V6 3l engine while consuming as a 2.2l common rail diesel engine.

Engine	V6 3.5 l gasoline	2.0 l T gasoline	**1.8 l T (IFP)**	2.2 l DCI
Max torque (Nm)	330	270	**310**	320
CO_2 (g/km)	250	220	**196**	190

Engine Issue was to reach a CO_2 emission of 195 g/km on NEDC cycle. Engine control issue was thus to assure accurate fuel/air equivalent ratio control during overall cycle. NEDC results with IFP downsizing demonstration car is above 195 g/km which is quite good considering a non-optimal calibration as on production car.

CO/NOx emissions

Goal was to reach EURO IV, even EURO V, emission standard as represented on next table.

Emission (g/km)	EURO IV	EURO V	**Results**
CO	1	1	**0.49**
NOx	0.08	0.06	**0.058**

From the first NEDC, CO emissions were not a problem, reaching easily EURO V level. On the other hand first NOx emissions were too high because of a bad exhaust catalyst conversion.

A first step to reduce NOx is to get a 1 Hz oscillation on fuel/air equivalent ratio measurement with amplitude above 0.005. It has been achieved by increasing PI controller parameters function of engine speed and adding oscillation on set point with an amplitude function of air mass *(cf. Fig. 22)*. A second step was to optimize steady-state equivalent ratio level for an optimal conversion between CO and NOx with a static correction on equivalent ratio set point function of air mass. A final calibration on rolling test bed permits to reach EURO V NOx emissions level.

HC emissions

Last issue, but not the least, is low HC emissions. Preliminary tests on engine test bed permits to find optimal steady-state settings to apply in order to limit HC emissions (spark advance, Equivalence ratio set point, injection phasing...).

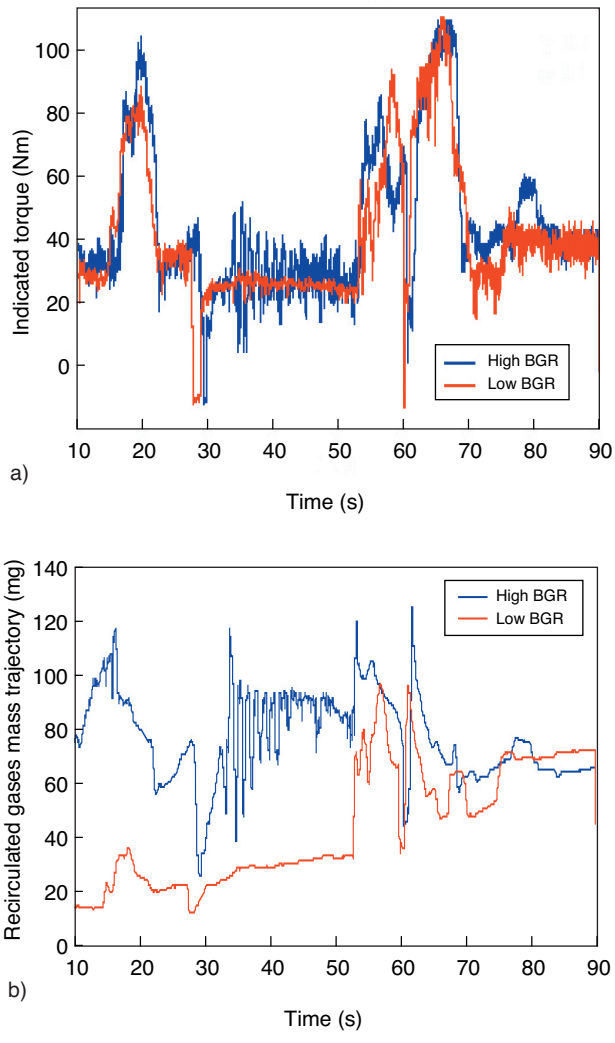

Figure 28

Burnt gases trajectory during warm-up on ECE cycle.

As we seen before, a control contribution is to be able to define an optimized residual burned gas trajectory during warm-up for getting low HC emissions while keeping stability.

Figure 28 illustrates the recirculated gases mass control ability. Two different trajectories have been tested: one coming from warm optimal setting with high burned gas ratio in order to limit HC emissions, and another with low burned gas ratio to improve stability. We can see that warm optimal trajectory in cold conditions leads to combustion instability, whereas the second, because of VCT uncrossing, get stability but HC emissions were not good enough.

This work is still in progress, but preliminary tests shows that an optimized residual burned gas trajectory function of temperature could lead to reduce HC emissions. One solution could be to constraint exhaust VCT position while RGM supervision reduces burned gas ratio (different intake VCT trajectory) in order to keep stability.

CONCLUSION

This paper has presented overall engine control development of a downsized spark ignition engine, from torque-based structure scheme tested in simulation to integration and calibration on *IFP* demonstration vehicle.

The purpose was to validate the propose approach and contribution: a torque control based on in-cylinder gases mass observation and non-linear control. We have seen impact of trapped air mass closed-loop observation, not only in air path in order to accuracy control air mass trapped, and thus torque, but also for an accurate AFR control. The recirculated gases mass optimization control offers the ability to control burned gas or scavenging independently of air mass control and to reach different set points while keeping air mass constant.

This physical approach makes it possible to separate the supervision from control. Air mass trapped in cylinder and recirculated gases mass trajectories are defined upstream in structure function of driver requests, warm-up strategies...

The good control performances on vehicle are very encouraging about this control approach and methodology. Further work will focus on improvement of air mass observation, especially dynamic aspects, and multivariable control of air path on optimized feasible trajectories.

ACKNOWLEDGEMENTS

The authors want to thank Boris Huart for his support in setting up software-in-the-loop and hardware-in-the-loop platforms and his help in control development and validation. We also want to thank Patricia Anselmi for her engine expertise, leading steady-state engine tests on test bed, and calibration work on vehicle.

REFERENCES

1 Lecointe, B. and Monnier, G. (2003) Downsizing a gasoline engine using turbocharging with direct injection. SAE Technical Papers, 2003-01-0542.

2 Corde, G. (2002) Le contrôle moteur, in *Contrôle commande de la voiture*, Gissinger, G. and Le Fort Piat, N. (Eds.), Hermès, Paris.

3 Albrecht, A., Corde, G., Knop, V., Boie, H. and Castagne, M. (2005) 1D simulation of turbocharged gasoline direct injection engine for transient strategy optimization. SAE Technical Papers, 2005-01-0693.

4 Menegazzi, P., Aubret, P. and Vernhes, P.-L. (2004) Conventional and Hybrid Vehicle Emission, Fuel Economy and Performance Analysis System Simulation. *FISITA 2004*, Barcelona, Spain.

5 Le Berr, F., Miche, M., Le Solliec, G., Lafossas, F.-A. and Colin, G. (2006) Modelling of a Turbocharged SI Engine with Variable Camshaft Timing for Engine Control Purposes. SAE Technical Papers, Toronto.

6 Colin, O., Benkenida, A. and Angelberger, C. (2003) A 3D Modeling of Mixing, Ignition and Combustion Phenomena in Highly Stratified Gasoline Engines. *Oil Gas Sci. Technol.*, **58**, 47-62.

7 Heywood, J.B. (1988) *Internal Combustion Engine Fundamentals*, McGraw Hill.

8 Sjöberg, J., Zhang, Q., Ljung, L., Benveniste, A., Delyon, B., Glorennec, P., Hjalmarsson, H. and Juditsky, A. (1995) Nonlinear black-box modeling in system identification: a unified overview. *Automatica*, **31**, 12, 1691-1724.

9 Norgaard, M., Ravn, O., Poulsen, N. and Hansen, L. (2000) *Neural Networks for modeling and control of Dynamics Systems*, Springer.

10 Colin, G., Chamaillard, Y., Bloch, G. and Corde, G. (2005) Neural Networks for Feedback Control. *IEEE*.

Final manuscript received in October 2006